Available online at www.sciencedirect.com
SCIENCE DIRECT®
Vision Research 46 (2006) 636–651
Vision Research
www.elsevier.com/locate/visres

Effect of myopia on visual acuity measured with laser interference fringes

Nancy J. Coletta *, Tonya Watson [1]

New England College of Optometry, 424 Beacon Street, Boston, MA 02115, USA

Received 24 February 2005; received in revised form 23 May 2005

Abstract

The aim was to determine how visual acuity is affected by myopia when optical factors of the eye are controlled. Grating acuity was measured with interference fringes to avoid the effects of aberrations, and ocular biometry was used to compensate for differences in retinal image size among subjects. Distance spectacle refractions ranged from +2.25 to −14.75 D. The retinal magnification factor (RMF) in mm/deg was computed for each eye from the distance refraction, central corneal power and ultrasound biometry. A forced-choice orientation discrimination method was used to measure acuity for high-contrast 543 nm laser interference fringes in three retinal locations: the fovea, and at 4 deg and 10 deg eccentricity in the temporal retina. Acuity, expressed in c/deg and adjusted for spectacle magnification, was not significantly correlated with refraction at any of the three retinal locations. When acuity was converted to retinal spatial frequency units (c/mm) via the RMF, acuity decreased with increasing myopia at all three retinal locations (significantly at the fovea and at 10 deg eccentricity). Retinal acuity values in highly myopic subjects (>6 D) are consistent with retinal sampling distances that are larger than published values of human cone or ganglion cell spacing. The results imply that a highly myopic eye has retinal neurons that are more widely spaced than normal, but the increased axial length enlarges the retinal image enough to compensate for the retinal stretching. The data are consistent with a retinal stretching model that primarily affects the posterior pole.

Keywords: Myopia; Refraction; Acuity; Laser interferometry; Retinal magnification; Optical quality

1. Introduction

Myopic subjects exhibit reduced visual acuity (Chui, Yap, Chan, & Thibos, 2005; Collins & Carney, 1990; Curtin, 1985; Strang, Winn, & Bradley, 1998) and contrast sensitivity at high spatial frequencies, (Comerford, Thorn, & Corwin, 1987; Fiorentini & Maffei, 1976; Liou & Chiu, 2001; Thorn, Corwin, & Comerford, 1986) compared to subjects with emmetropia. The acuity deficit in myopia can be attributed to several factors, such as the optics of correcting lenses, coarsened neural sampling due to retinal stretching and to the optical quality of the myopic eye. It is apparent that spectacle correction reduces acuity in myopia because visual acuity improves when myopic subjects are corrected with contact lenses (Collins & Carney, 1990; Liou & Chiu, 2001; Strang et al., 1998). This effect is partially due to spectacle minification of the retinal image (Applegate & Howland, 1993; Strang et al., 1998; Chui et al., 2005), but is also related to the optical quality of spectacles (Collins & Carney, 1990). Myopia above about 4 D is due mainly to an increase in the axial length of the eye (Curtin, 1985) and retinal image magnification from the eye's increased axial length should balance the minification from spectacles (i.e., Knapp's law; Bennett & Rabbetts, 1998; Bradley, Rabin, & Freeman, 1983; Chui et al., 2005; Tunnacliffe, 1993). Strang et al. (1998) point out

* Corresponding author. Tel.: +1 617 236 6253; fax: +1 617 424 9202.
E-mail address: colettan@neco.edu (N.J. Coletta).
[1] Present address: School of Optometry, University of California, Berkeley, CA 94720, USA.

0042-6989/$ - see front matter © 2005 Elsevier Ltd. All rights reserved.
doi:10.1016/j.visres.2005.05.025

that axial myopes corrected with contact lenses should have better acuity than emmetropes, due to the axial length magnification in myopia. However, with contact lens correction, visual acuity in myopes either matches or is slightly worse than the level obtained for emmetropia (Liou & Chiu, 2001; Strang et al., 1998). This has been interpreted as evidence for a residual neural deficit in myopia (Strang et al., 1998) which is most likely associated with retinal stretching of the myopic eye (Bradley et al., 1983; Chui et al., 2005; Curtin & Karlin, 1971; Kramer, Shippman, Bennett, Meininger, & Lubkin, 1999; Romano & von Noorden, 1999; Strang et al., 1998; Winn et al., 1988).

Another factor that could account for reduced visual acuity in myopia is that the optical quality of myopic eyes may be worse than that of emmetropic eyes. A number of studies indicate that myopic eyes have greater ocular aberrations than emmetropic eyes (Applegate, 1991; Carkeet, Luo, Tong, Saw, & Tan, 2002; Coletta, Marcos, Wildsoet, & Troilo, 2003; Collins, Wildsoet, & Atchison, 1995; He et al., 2002; Marcos, Moreno-Barriuso, Llorente, Navarro, & Barbero, 2000; Paquin, Hamam, & Simonet, 2002). Contact lens correction in myopia could introduce additional aberrations, either while the lenses are in place (Dorronsoro, Barbero, Llorente, & Marcos, 2003; Hong, Himebaugh, & Thibos, 2001; Lu, Mao, Qu, Xu, & He, 2003) or after contact lens removal (Coletta & Moskowitz, 2003). Since the previous studies of acuity and contrast sensitivity in myopia were performed with conventional stimuli that are viewed through the eye's optics, the visual acuity deficit in myopia could be related to the optical quality of the myopic eye with its refractive correction.

The main objectives of this experiment were to determine whether visual acuity is reduced in myopia when the deleterious effects of optical aberrations are minimized and when the measured acuity limits are compensated for differences in retinal image size among subjects. To avoid the effects of optical aberrations that might increase in myopia, the grating acuity stimuli were high-contrast laser interference fringes formed directly on the retina. This technique allows the subject to view grating patterns that are relatively unaffected by optical quality and defocus (Campbell & Green, 1965; Frisen & Glansholm, 1975; Williams, 1985a). While a previous study had shown no effect of refractive error on interferometric acuity, that study combined data for myopic and hyperopic refractions (Geddes, Patel, & Bradley, 1990). The eye's refractive correction (Williams, 1985a) and its axial length (Williams, 1988) affect the retinal spatial frequency of interference fringes. To compensate for differences in the retinal image size across subjects, we used ocular biometry and a schematic eye model to calculate each subject's retinal magnification factor (RMF) in mm/deg. Interferometric acuity in cycles/deg could then be converted to cycles/mm on the retina, allowing an estimate of acuity in units of retinal spacing.

Acuity measured by interferometry is generally considered to be limited by the spatial sampling rate of cones in the fovea (Green, 1970; Williams, 1985b; Williams & Coletta, 1987), and by the density of retinal ganglion cells in the periphery (Anderson, Wilkinson, & Thibos, 1992; Frisen & Frisen, 1976; Green, 1970; Thibos, Cheney, & Walsh, 1987). Since retinal stretching in myopia may not be uniform across the visual field (Strang et al., 1998; Troilo, 1998; Chui et al., 2005; Vera-Diaz, McGraw, Strang, & Whitaker, 2005), we measured interferometric acuity in the fovea, parafovea and near periphery and compared the results to anatomical estimates of cone and retinal ganglion cell spacing.

2. Methods

2.1. Subjects

Measurements were made on 18 adult subjects recruited from the faculty, staff and students of the New England College of Optometry. Subjects' ages ranged from 22 to 47 years with an average of 26.2 years. The right eye was tested in all but three subjects, for whom the left eye was dominant. Distance spectacle refractive corrections ranged from +2.25 to −14.75 D (spherical equivalent in the 14 mm vertex plane) with astigmatism less than 1.25 D. Exclusion criteria were ocular pathology, amblyopia, or previous ocular surgery. This research adhered to the tenets of the Declaration of Helsinki. The experiment was approved by the Institutional Review Board of the New England College of Optometry and informed consent was obtained from all subjects after explanation of the nature and possible consequences of the study.

2.2. Computation of retinal magnification from ocular biometry

The retinal magnification factor was estimated for each eye, using a three-surface schematic eye model that has the refractive indices of the Gullstrand–Emsley schematic eye (Bennett, 1988; 1.333 for the aqueous and vitreous humors and 1.416 for the lens), but is based on the individual subject's distance spherical equivalent refraction, central corneal power, and A-scan ultrasound measurements. The distance refraction was measured with a Topcon RM-8000 Auto-Refractometer, which uses a fogging technique to keep accommodation relaxed and has been shown to provide excellent agreement with subjective refraction (Pesudovs & Weisinger, 2004). Five measurements were made per eye and the average of the five readings was used as the distance spectacle refraction in the 14 mm vertex plane. Central corneal power

was measured with a Humphrey Atlas 995 corneal topographer and was typically averaged from four images. The ultrasound measurements of anterior chamber depth, lens thickness and vitreous chamber depth were made with a Sonometrics A-scan apparatus, set for a tissue velocity of 1550 m/s. Measurements were taken through the subject's eyelid; this has been shown to be an accurate and repeatable method (Laws, Laws, Wood, & Clark, 1998). During measurements, the fellow eye of the subject was used to direct fixation and control accommodation by keeping a distant target in focus. Distances from the posterior corneal surface to the anterior lens, posterior lens and inner limiting membrane of the retina were recorded. Five measurements were taken per eye and then averaged. Since through-the-lid measurements do not allow measurement of the corneal thickness, the cornea was estimated to be 0.544 mm thick, a figure that was based on a survey of published ultrasound studies (Doughty & Zaman, 2000). Axial length is defined as the sum of the anterior chamber depth (including the estimated corneal thickness), lens thickness, and vitreous chamber depth, from the posterior lens to the internal limiting membrane of the retina.

The surface powers of the crystalline lens were calculated for each eye by the method described in Royston, Dunne, and Barnes (1989), which is based on Bennett's (1988) method for determining the power of the crystalline lens without phakometry. The experimental error in phakometry is greater than the error in Bennett's method (Dunne, Barnes, & Royston, 1989). The positions of the cardinal points for the uncorrected eye were then calculated by paraxial optics formulae and the step-along method (Tunnacliffe & Hirst, 1996), using a distant target (zero Diopters of vergence incident at the cornea), the eye's measured axial dimensions, central corneal power and the estimated surface powers for the crystalline lens. From the resulting posterior nodal point distance (PND, the distance from the posterior nodal point, N', to the retina in mm), the RMF in mm/deg for each uncorrected eye was calculated as follows:

$$\mathrm{RMF}_{\mathrm{unc}} = \mathrm{PND} * (\tan 1\ \mathrm{deg}). \tag{1}$$

This value, $\mathrm{RMF}_{\mathrm{unc}}$, represents the diameter of retina in mm covered by a 1 deg diameter stimulus when the subject's eye is uncorrected. Most of the subjects wore refractive correction during the acuity measurements. Correcting lenses change the angle of the incident light at the eye with the result that negative spectacle lenses (and to a lesser extent, negative contact lenses) minify the retinal image compared to the uncorrected case (Applegate & Howland, 1993; Chui et al., 2005; Strang et al., 1998; Tunnacliffe, 1993). Since spectacle magnification represents the ratio of the corrected to the uncorrected retinal image size (Tunnacliffe, 1993), RMFs for spectacle-corrected and contact lens-corrected conditions were determined for every subject from the $\mathrm{RMF}_{\mathrm{unc}}$ and the appropriate magnification for each correction condition. To calculate the spectacle magnification for each eye, the distance from the anterior cornea to the entrance pupil (d_1') was first calculated from the anterior chamber depth (d_1) and, assuming the correcting spectacle lens was thin, the power factor of the spectacle magnification was calculated (Tunnacliffe, 1993). Magnification for the spectacle-corrected condition (M_{sp}) is thus given by

$$M_{\mathrm{sp}} = 1/(1 - (h + d_1') * F_{\mathrm{sp}}), \tag{2}$$

where h is the spectacle vertex distance to the anterior cornea and F_{sp} is the distance spectacle correction. For spectacle-corrected myopes, M_{sp} will be less than 1, resulting in minification of the retinal image. For these calculations, h was set at 14 mm since the distance refractions were referenced to that vertex distance. Retinal magnification for the spectacle-corrected condition ($\mathrm{RMF}_{\mathrm{sp}}$) is then given by:

$$\mathrm{RMF}_{\mathrm{sp}} = \mathrm{RMF}_{\mathrm{unc}} * M_{\mathrm{sp}}. \tag{3}$$

Magnification for the contact lens-corrected condition (M_{cl}) is given by:

$$M_{\mathrm{cl}} = 1/(1 - d_1' * F_{\mathrm{cl}}), \tag{4}$$

where F_{cl} is the distance contact lens correction (Tunnacliffe, 1993). Retinal magnification for the contact lens-corrected condition ($\mathrm{RMF}_{\mathrm{cl}}$) is then given by:

$$\mathrm{RMF}_{\mathrm{cl}} = \mathrm{RMF}_{\mathrm{unc}} * M_{\mathrm{cl}}. \tag{5}$$

2.3. Interference fringe acuity

Sinusoidal interference fringes were produced with a 543 nm helium–neon laser, and fringe contrast, spatial frequency and orientation of the fringes were controlled by a computer (Coletta & Sharma, 1995). Light from the laser was divided into two beams; each traveled through an acousto-optic modulator (AOM) that flickered the laser beam at approximately 500 Hz. Fringe presentation was controlled by adjusting the relative temporal phase of the pulses of the two beams; the fringe contrast was 100% when the pulse trains were in phase, and 0% when the pulses were out of phase. To control fringe spatial frequency and orientation, the beams traveled in opposite directions through a 16 mm thick optical flat that could be rotated about two orthogonal axes. The flat was positioned with computer-controlled microstepping motors that provided spatial frequency resolution of 0.16 c/deg per microstep. The beams were then collimated and recombined to form interference fringes. A final Maxwellian view lens focused the beams to two points located near the subject's entrance pupil; the beams diverged from these points to form fringes on the retina. A field stop in the final collimated beam of

the interferometer was used to confine the fringes to a circular patch. To ensure that spatial frequencies were equal for both vertical and horizontal fringe orientations, a spatial frequency calibration was performed before each test run, by projecting the fringe pattern in a 1 deg circular patch on a wall and counting fringes for both vertical and horizontal orientations at several spatial frequencies up to 12 c/deg. This reason for this procedure was to ensure that possible small misalignments of optical components did not introduce additional fringe cycles that would alter the fringe spatial frequency; introduction of additional cycles would create a particularly large error at low spatial frequencies. If the fringe counts differed, adjustments were made to the interferometer to equalize frequencies at both orientations.

Absorptive neutral density filters were placed in the interferometer to adjust the mean retinal illuminance of the fringes to 300 photopic trolands. The optical system was baffled to contain stray light. A 1 deg diameter circular fringe patch was used for testing acuity in the fovea and at 4 deg eccentricity in the temporal retina. For testing at 10 deg eccentricity in the temporal retina, the circular patch was 2 deg in diameter. A second Maxwellian view channel in the optical system consisted of a Tungsten light source and a 543 nm interference filter. This channel provided an approximately 8.5 deg diameter annulus of incoherent light that surrounded the fringe patch. For foveal testing, subjects fixated the center of the fringe patch; for the 4 deg test location, subjects fixated a black cross located 0.25 deg inside the edge of the surrounding annulus; for the 10 deg test location, subjects fixated a red blinking LED that subtended about 0.25 deg diameter.

Subject alignment in the interferometer ensured that the eye was in a fixed reference position relative to the two laser focus points. Subjects were positioned in the apparatus with a chin rest mounted on a three-axis stage and a head rest with temple supports was used to keep the subject's head steady. The subject's pupil center was aligned horizontally and vertically with the optical axis of the interferometer, using an infrared source and a CCD camera that was conjugate with the plane of the laser focus points. For eccentric viewing conditions, subjects fixated the appropriate fixation mark during the alignment procedure. Positioning of the subject's eye along the optical axis of the interferometer (z-axis) was achieved by focusing the subject's iris in the pupil camera, which placed the laser focus points about 4 mm in front of the eye's nodal plane. Interference fringe magnification varies with fore and aft positioning by $1 - (d/k)$, where d is the fore and aft separation between the focus point and the eye's nodal point, and k is the position at which the eye is focused (Williams, 1988). The eyes of all but three subjects were conjugate with infinity during the experiments, so fringe magnification was unaffected by fore and aft position in the majority of subjects. The three remaining subjects were tested without distance correction, but because their refractive errors were small (−1.87, −1.00, and +2.25 D), the lack of correction would have affected fringe magnification by less than 1%. Uncorrected refractive error does not affect fringe contrast but results in doubling of the field stop which defines the edge of the fringe patch. In these cases, the field stop position was adjusted until the subject reported that the laser fringe patch appeared single.

The acuity limit was estimated from psychometric functions of orientation discrimination, using a single-interval, two-alternative forced-choice method of constant stimuli. The subjects viewed the fringes monocularly in a darkened room. On a given stimulus trial, a 100% contrast vertical or horizontal fringe was presented for a duration of 200 ms, signaled by a simultaneous tone. The subject's task was to choose the orientation and enter the response using a joystick. This process was repeated for various spatial frequencies, in 5 c/deg steps for the fovea and 4 deg eccentricity, and in 1 c/deg steps at 10 deg eccentricity. Up to four randomly interleaved spatial frequencies, with 10 trials at each orientation, were tested at a time; each group of frequencies was tested twice, yielding a total of 40 trials per frequency. Psychometric functions were plotted as the proportion correct as a function of spatial frequency. A cumulative Weibull function, modified to fit psychometric data that fall from 100% to 50% correct (guessing), was fit to the data using a least-squares method. The function was:

$$y = \frac{2 - e^{\left(-\frac{\eta}{x}\right)^{\beta}}}{2}, \tag{6}$$

where x is the spatial frequency of the interference fringe in cycles per degree, y is the proportion correct, η is the scale parameter and β is the shape parameter. The acuity limit was defined as the spatial frequency corresponding to the 0.75 correct level on the curve fit. The proportion correct was averaged for both vertical and horizontal orientations to derive the resolution limits shown in the results. However, we also performed a separate analysis of psychometric functions for the individual vertical and horizontal orientations to search for evidence of anisotropy, which could be larger in myopia (Vera-Diaz et al., 2005).

Spectacle correction alters interference fringe spatial frequency (Williams, 1985a) and we verified this effect empirically by placing a series of trial lenses at a vertex distance of 15 mm in front of the laser focus points and measuring the change in point separation. Because the trial lenses are in a convergent beam, minus lenses increase the point separation (and therefore increase the fringe spatial frequency, analogous to minimizing the

retinal image) and positive lenses decrease the point separation (decrease the fringe spatial frequency or magnify the retinal image). The empirical effect of trial lens power on fringe spatial frequency matched the prediction from spectacle magnification for the tested vertex distance. Therefore, the acuity limits obtained for subjects who wore correction during the experiment were compensated for spectacle or contact lens magnification by dividing the acuity limit by the appropriate magnification value obtained from Eq. (2) or (4), respectively, depending upon the subject's test condition. Eight subjects wore contact lenses during measurements and six wore spectacles; of the remaining subjects, one was an emmetrope and three had small refractive errors as described above. For subjects who wore spectacles during acuity measurements, spectacle lens powers were checked by lensometry and these spectacle powers were used to adjust the acuity limits. The same retinal magnification factors were used for each retinal location since the eye's retinal magnification is nearly constant over the central 20 deg of the visual field (Drasdo & Fowler, 1974) and the variation in spherical equivalent refraction from the fovea to 10 deg nasal visual field is typically under a 0.5 D (Atchison, Scott, & Charman, 2003).

3. Results

3.1. Biometry and retinal image magnification

The subjects' axial lengths and corneal powers are compared to their refractive errors in Fig. 1. Axial lengths ranged from 21.14 to 26.81 mm and central corneal powers ranged from 41.95 to 46.80 D. Axial length and corneal power both increased with increasing myopia, in agreement with previous studies (Carney, Mainstone, & Henderson, 1997; Goss, Cox, Herrin-Lawson, Nielsen, & Dolton, 1990; Grosvenor & Scott, 1994; Van Alphen, 1961). There was a significant correlation between axial length and spectacle refraction ($r = 0.91$; $p < 0.0001$) while the relationship between corneal power and spectacle refraction did not quite reach significance ($r = 0.45$; $p = 0.058$). Thus, the refractive errors of our subjects were primarily axial in nature but the tendency for variation in corneal power suggests that optical parameters of the eyes were not constant across subjects.

Retinal magnification factors, computed for each subject for each possible viewing condition, are shown as a function of distance spectacle refraction in Fig. 2. The RMF_{unc} values are shown as filled circles, RMF_{cl} values are shown as open circles and RMF_{sp} values are shown as open diamonds. Our estimate of the RMF for the emmetropic eye (0.272 mm/deg) is very similar to published estimates of the RMF for the posterior pole in wide-field schematic eyes (Drasdo & Fowler, 1974; Holden & Fitzke, 1988). As expected, the RMF_{unc} values show that uncorrected myopic eyes have significantly larger retinal images than emmetropic eyes ($r = 0.94$; $p < 0.0001$), which is evidence of axial length magnification in myopia. The RMF_{sp} values show that spectacle correction results in relative minification of the retinal image in myopic eyes. However, even with spectacle correction in the 14 mm plane, the myopes have significantly larger retinal images than emmetropes ($r = 0.52$; $p = 0.028$). To achieve perfect compensation of the axial length magnification by spectacles, i.e., to obtain a slope of zero for the RMF_{sp} data, our subjects would need a spectacle vertex distance of 19.2 mm in front of the cornea.

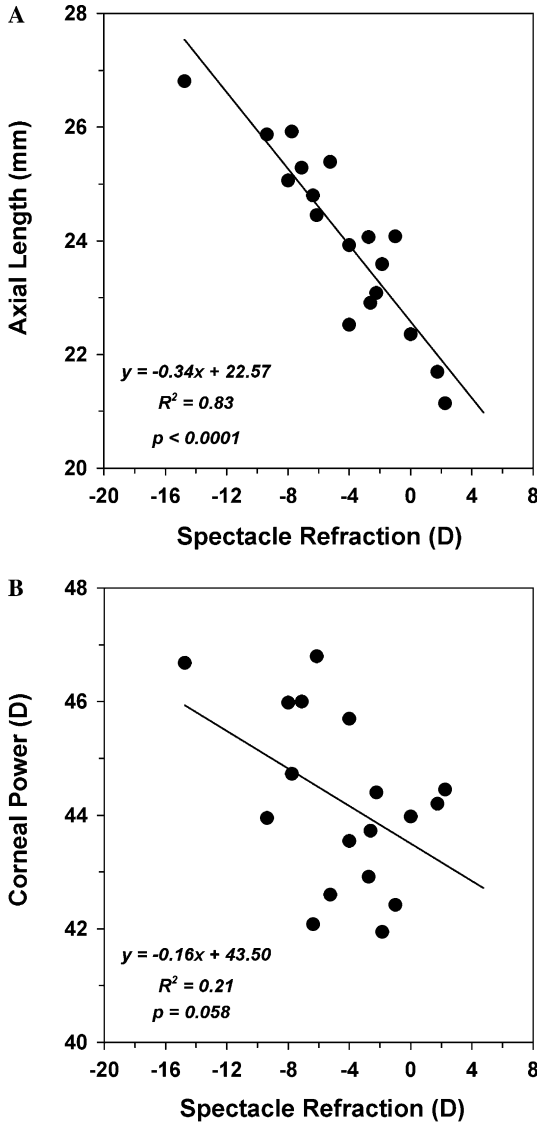

Fig. 1. Axial length (A) and central corneal power (B) of the subjects' eyes plotted as a function of their spherical equivalent distance spectacle refraction in Diopters. Solid lines in both plots are linear regressions to the data.

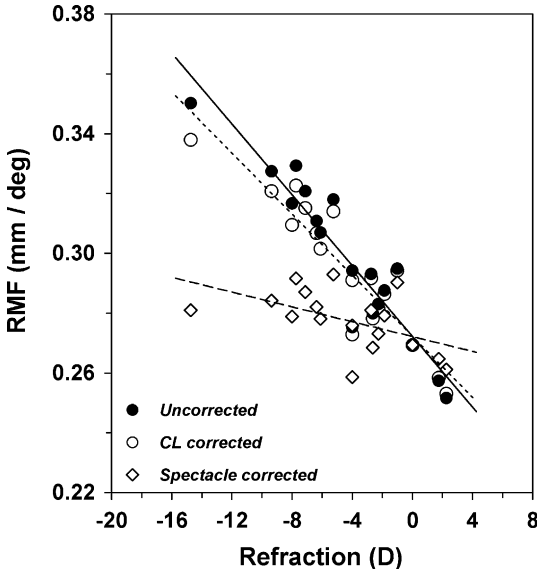

Fig. 2. The retinal magnification factor (RMF), in mm/deg, computed for each eye and plotted as a function of spherical equivalent distance spectacle refraction in Diopters. The uncorrected values (filled circles) were obtained from the uncorrected schematic eye constructed for each subject, while the contact lens-corrected RMF (open circles) and spectacle-corrected RMF (open diamonds) were calculated by multiplying the uncorrected values by each individual's contact lens or spectacle magnification, respectively. Lines are linear regressions to the data.

3.2. Acuity and refractive error

As stated above, if the subject wore refractive correction during the measurement, the acuity limit derived from each psychometric function was divided by the subject's magnification factor (either M_{sp} or M_{cl}) appropriate for their testing condition. These compensated acuity values allow us to compare visual performance across subjects without the effect on retinal image size of the refractive correction. The compensated acuity limits in angular units of spatial frequency (c/deg) are plotted against the distance spectacle refraction in Fig. 3A for all three retinal locations. Data are shown on a logarithmic ordinate to better compare slopes at the three retinal eccentricities. Fig. 3A indicates that interferometric acuity is not affected by the degree of myopia.[2] The slope of the linear regression is not significant at any retinal location ($p = 0.22$ for the fovea, $p = 0.98$ for 4 deg eccentricity and $p = 0.18$ for 10 deg eccentricity). Overall, the data indicate that, when optical factors are minimized, angular acuity is slightly reduced in myopia but not by a significant amount.

Fig. 3B shows the same interferometric acuity data re-plotted in units of c/mm on the retina. These data,

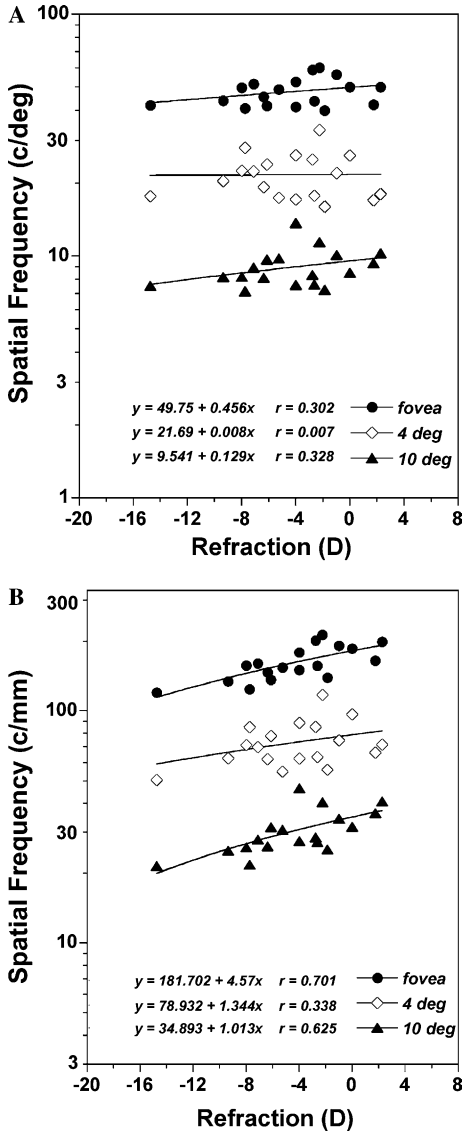

Fig. 3. (A) Interferometric acuity in angular units of spatial frequency (c/deg) plotted as a function of spherical equivalent distance spectacle refraction in Diopters, for the fovea (filled circles), 4 deg eccentricity in temporal retina (open diamonds) and 10 deg eccentricity in temporal retina (filled triangles). Acuity data were estimated from the 75% correct level of a psychometric function of orientation discrimination, averaged for vertical and horizontal interference fringes. Acuity values shown here have been compensated for spectacle or contact lens magnification in those subjects who wore correction during the measurements. (B) Interferometric acuity in units of retinal spatial frequency (c/mm) plotted as a function of spherical equivalent distance spectacle refraction in Diopters, for the fovea (filled circles), 4 deg eccentricity in temporal retina (open diamonds) and 10 deg eccentricity in temporal retina (filled triangles). Linear regression equations are given in the symbol legend order.

termed retinal acuity, allow us to compare visual performance across subjects without the effects on retinal image size of both axial length and the refractive correction. The retinal acuity values were obtained by dividing the uncompensated acuity limit in c/deg by the RMF value from Eq. (1), (3), or (5) appropriate

[2] Our preliminary data on a smaller subject sample implied that myopic eyes had higher acuity than emmetropic or hyperopic eyes (Watson et al., *IOVS, 43*, 2002:ARVO E-abstract 2005).

for each subject's experimental viewing condition. (The same results would be obtained by dividing the compensated acuity in c/deg by the uncorrected RMF for each subject). When the data are plotted in retinal acuity units, acuity significantly decreases with increasing myopia in the fovea ($r = 0.701$; $p = 0.0012$) and at 10 deg eccentricity ($r = 0.63$; $p = 0.0055$). At 4 deg eccentricity, the slope of the retinal acuity vs. refraction regression was not significant ($r = 0.34$; $p = 0.17$) but it was steeper than the corresponding regression line for angular acuity units in Fig. 3A. Furthermore, the slopes of the regression lines are similar at all three retinal locations on the logarithmic scale, which implies that the effect of myopia on acuity is fairly uniform out to 10 deg eccentricity. While it appears that the data point from the most highly myopic subject might have created the significant effects at the fovea and 10 deg eccentricity, the linear regressions at the fovea ($r = 0.64$; $p = 0.0056$) and at 10 deg ($r = 0.57$; $p = 0.017$) are still significant when this subject is excluded.

Retinal stretching in the near periphery of myopic eyes is reported to be anisotropic, based on the increased magnitude of the horizontal–vertical illusion in myopia (Vera-Diaz et al., 2005). We examined the separate horizontal and vertical fringe data to determine whether any meridional biases in retinal acuity were more pronounced in myopia. We determined 75% acuity limits from psychometric functions for the individual horizontal and vertical stimuli; the average of these acuity limits was in good agreement with the acuity derived by averaging the percentage correct at the two orientations ($p < 0.0001$ for each retinal location). When each subject's percent difference between horizontal and vertical retinal acuity was plotted against their refractive error, the linear regressions were not significant at any retinal location (fovea, $p = 0.74$; 4 deg eccentricity, $p = 0.29$; 10 deg eccentricity, $p = 0.97$). The percent difference in horizontal and vertical acuity was also not significantly different in t tests when the subjects were grouped into myopia greater or lesser than 6 D (fovea, $p = 0.23$; 4 deg eccentricity, $p = 0.11$; 10 deg eccentricity, $p = 0.46$). Thus we found no evidence for increased horizontal–vertical anisotropy in myopia in our retinal acuity data. It is possible that the exaggerated horizontal–vertical anisotropy in the periphery of myopic eyes (Vera-Diaz et al., 2005) is not evident with small grating patches but requires judgments of distance over longer retinal intervals.

The different pattern of results for retinal acuity (c/mm) and angular acuity (c/deg) in Fig. 3 implies that axial length magnification provides some benefit for acuity in myopia. Fig. 4 shows the foveal acuity data in either retinal units (filled symbols—left ordinate) or angular units (open symbols—right ordinate), plotted on ordinate scales that cover the same factor of 2.4 from the minimum to the maximum ordinate value and are adjusted to coincide for emmetropia. With increasing myopia, angular acuity decreases at a shallower rate than retinal acuity. Since both sets of acuity values have been compensated for variation in retinal image size due to spectacle or contact lens correction, the difference between the slopes of the two linear regressions indicates the effect of axial length magnification in myopia.

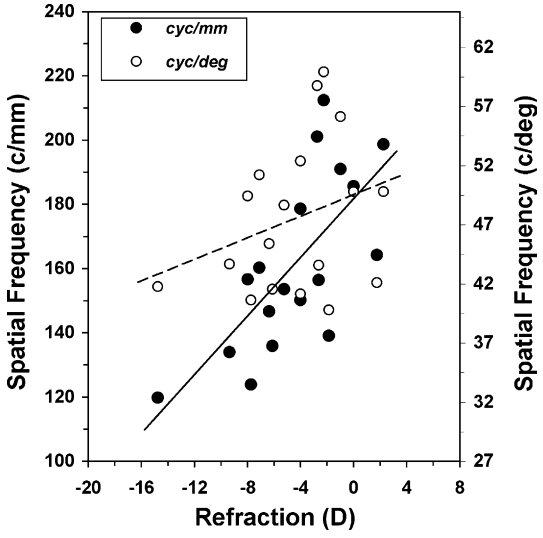

Fig. 4. Foveal interferometric acuity results are shown in retinal spatial frequency units of c/mm (solid symbols, left hand ordinate) and angular units of c/deg (open symbols, right hand ordinate). Solid line is the linear regression to the retinal acuity and dashed line is the linear regression to the angular acuity. The vertical scales for each acuity type are adjusted to coincide for emmetropia, using a 0.272 mm/deg retinal magnification factor, and both overall vertical scales cover a factor of 2.4 in acuity.

4. Discussion

Interferometric visual acuity was not reduced significantly in myopia when the acuity was expressed in angular units and compensated for spectacle magnification, which implies that previous reports of lowered acuity in myopia may have been due to optical factors. Our interferometric acuity data are compared in Fig. 5 to the results of two previous studies of acuity in myopia; both of these studies were performed with subjects who wore spectacles and viewed conventional stimuli. The data from Strang et al. (1998) were collected with high-contrast LogMAR letter acuity charts, and the data from Chui et al. (2005) were collected with gratings and a forced-choice orientation discrimination paradigm. In all three panels, the figure compares foveal acuity in spatial frequency units against the distance spectacle refraction. Fig. 5A compares results from the three studies for subjects who are spectacle-corrected and whose acuity values have not been compensated for spectacle magnification. Fig. 5B compares the same results when acuity has been compensated for spectacle

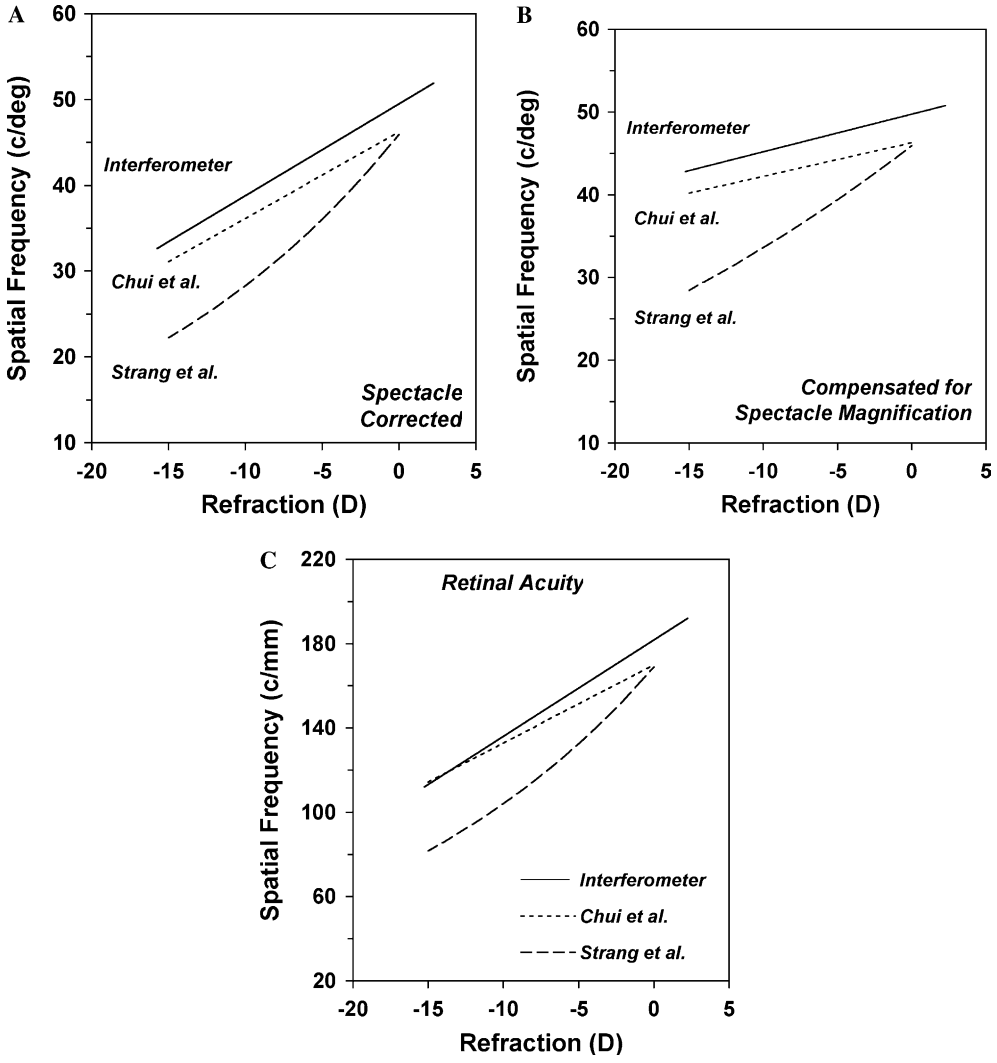

Fig. 5. Comparison of foveal acuity obtained in this study to foveal acuity obtained in two other studies that used conventional targets viewed through the optics of the eye. In each panel, acuity is plotted as a function of the distance spherical equivalent refraction in Diopters. (A) Angular acuity in c/deg obtained with spectacle correction but not compensated for the minifying effects of spectacles. The solid line is the linear regression to the interferometric angular acuity from Fig. 3A, in which the compensated acuity values have been multiplied by each subject's spectacle magnification factor (M_{sp}). The dotted line is the linear regression to acuity measured with gratings from the study of Chui et al. (2005) (their Fig. 3, fovea). The dashed line is the linear regression to acuity measured with letter charts from the study of Strang et al., 1998 (their Fig. 4, converted to spatial frequency units from LogMAR). (B) Angular acuity in c/deg as in (A), but compensated for the minifying effects of spectacles. The solid line is the linear regression to the compensated interferometric angular acuity in Fig. 3A. The dotted line is the linear regression to foveal acuity in the Chui et al.'s (2005) study, compensated for spectacle magnification (their Fig. 6). The dashed line was obtained by dividing the Strang et al.'s (1998) spectacle-corrected acuity values shown in (A) by the spectacle magnification factor calculated for the 15 mm spectacle vertex and 3.68 mm entrance pupil distance used in that study. (C) Retinal acuity in c/mm. The solid line is the linear regression to the interferometric retinal acuity in Fig. 3B. For the studies with conventional targets, acuity in c/deg from (A) was converted to c/mm via a fixed RMF of 0.272 mm/deg. The dotted line is the retinal acuity from Chui et al. (2005) and the dashed line is retinal acuity from Strang et al. (1998).

magnification, and Fig. 5C compares the three studies when acuity has been converted to retinal units of c/mm.

Fig. 5A illustrates the actual angular acuity that would be obtained with spectacle correction, including the minifying effect of spectacle lenses in myopia. The solid line in Fig. 5A is a linear regression to our foveal interferometric acuity values that are uncompensated for spectacle magnification; since not all of our subjects wore spectacles during testing, these values were obtained by multiplying the compensated acuity values in Fig. 3A by each subject's spectacle magnification. The linear regression to these data ($y = 1.061x + 49.48$; $r = 0.613$; $p = 0.007$) shows that there is a significant reduction in interferometric acuity in myopia when the interference fringes are minified by minus spectacles. The dotted line is the linear regression from Fig. 3 of Chui et al. (2005) and the dashed line is a linear regression from Fig. 4 of Strang et al. (1998); the dashed line is curved because the original regression was fit to acuity in log units and we have converted the LogMAR values

to a linear spatial frequency scale. The slopes of the uncompensated acuity regressions are statistically significant in all three studies, indicating that spectacle-corrected angular acuity worsens with increasing myopia. This confirms that optical minification of the retinal image by minus-powered spectacles does result in decreased acuity in myopia.

Fig. 5B provides an estimate of the potential angular acuity that could be achieved in myopia if a non-minifying refractive correction were used. The solid line is the regression to our foveal compensated interferometric acuity from Fig. 3A. The dotted line is the linear regression from Fig. 6 of Chui et al. (2005); these compensated acuity limits are described in that study as the spatial frequencies of the "virtual stimulus." The dashed line was obtained by dividing the Strang et al.'s (1998) spectacle-corrected acuity values shown in Fig. 5A by spectacle magnification calculated for the 15 mm spectacle vertex and 3.68 mm entrance pupil distance used in that study. In both studies that used grating stimuli (our study and Chui et al., 2005), myopia did not have a significant effect on foveal angular acuity when it was compensated for spectacle magnification. Acuity obtained with letter charts (dashed line in Fig. 5B) appears to be worse in myopia even after compensation for the minifying effect of spectacles.

In Figs. 5A and B, both sets of conventional acuity data coincide for subjects with emmetropia, and both are lower than the interferometric acuity for emmetropia. This difference reflects the detrimental effect of the eye's optical quality. The conventional acuity may have been lowered by both monochromatic and chromatic aberrations of the eye, since the conventional studies both employed white light stimuli. One would expect to see an increasing separation of the interferometric and conventional acuity data sets with increasing myopia if the optical quality of the eye worsened in myopia. While this relationship is apparent for letter acuity, the interferometric and conventional grating acuity regressions have nearly the same slopes in both Figs. 5A and B. The latter two data sets were collected with similar stimuli and forced-choice methods, so the additional deficit in letter acuity in myopia may be due to factors other than optical quality. Thus, there does not appear to be evidence in Fig. 5 that the optical quality of the eye worsens with increasing myopia, which would be consistent with several studies of aberrations (Cheng, Bradley, Hong, & Thibos, 2003; Llorente, Barbero, Cano, Dorronsoro, & Marcos, 2004; Porter, Guirao, Cox, & Williams, 2001). However, the relationship between ocular aberrations and visual acuity is a complicated issue that is the subject of current scrutiny (e.g., Cheng, Bradley, & Thibos, 2004; Marsack, Thibos, & Applegate, 2004) and the aberrations of myopic eyes conceivably could have a larger effect on letter acuity than on grating acuity.

Fig. 5C compares the results from the three studies when acuity has been converted to retinal units of c/mm. Retinal acuity should allow a comparison of acuity across studies without the effects on the retinal image size of both axial length and the refractive correction, but retinal acuity obtained with conventional targets still includes any effects of the eye's optical quality. The solid line is the regression to our foveal data in Fig. 3B. Spectacle-corrected angular acuity from the other two studies in Fig. 5A was converted to retinal acuity units assuming a fixed RMF of 0.272 mm/deg, which is the value that we had determined for emmetropia. This conversion maintains the same relative positions of the three data sets for emmetropia and assumes that spectacle minification would perfectly balance axial length magnification in myopia. This assumption was used for the conversion to retinal acuity in the Chui et al.'s (2005) study.[3] Use of a fixed RMF could, however, result in an over-estimation of retinal acuity in highly myopic subjects. We found that the retinal image size in a spectacle-corrected myopic eye is still relatively magnified compared to an emmetropic eye, even though spectacles minify the retinal image in a myopic eye compared to its uncorrected state (Fig. 2). Had we used our emmetropic RMF to convert angular to retinal acuity in our study, we would have over-estimated retinal acuity in myopia. This may explain why the slope of retinal acuity from the Chui et al.'s study is shallower than the interferometric retinal acuity, causing the two data sets to coincide at a high level of myopia. Nonetheless, all three data sets indicate that myopic subjects have lower foveal retinal acuity than emmetropic subjects.

As observed for angular acuity, myopes have relatively lower retinal acuity for letter targets than for gratings. The discrepancy between the results for gratings and letters may be due to the crowding effect, in which acuity is worse for strings of letters or full charts than it is for single letters (e.g., Hess, Dakin, & Kapoor, 2000; Morad, Werker, & Nemet, 1999). The crowding effect could be more evident with increasing myopia if the lowered acuity in highly myopic subjects is considered as a form of refractive amblyopia (Fitzgerald, Chung, & Krumholtz, 2005; Romano, 1988). Even though our myopic subjects had not been diagnosed clinically with amblyopia, their relatively lower retinal acuity in Fig. 3B could be considered as a sub-clinical form of amblyopia. The crowding effect of letter charts is enhanced in amblyopia; for

[3] Chui et al. (2005) used a constant RMF of 0.262 mm/deg; this RMF value would raise their regression line in Fig. 5C so that it coincides with the interferometric retinal acuity at a level of −7 D of myopia. The Strang et al.'s (1998) study used an RMF value of 0.291 mm/deg for emmetropia; this value would adjust their data down by a small amount, so that it coincides with the interferometric data at about +5 D of hyperopia.

example, in the Morad et al.'s (1999) study, normal control subjects showed a 1.14 times worse VA with letter charts as opposed to single letters, while anisometropic (refractive) amblyopes showed a 1.31 times worse VA with charts compared to single letters. Another possibility for the discrepancy between the results with letters and gratings is that gratings are resistant to undersampling when a sampling array is irregular, or characterized by variability in the sample spacing (Geller, Sieving, & Green, 1992; Williams & Coletta, 1987). It is possible that a stretched myopic retina may have a more irregular sampling array than a normal retina; in that case, a myope could have relatively better acuity for gratings than for letters because gratings are repetitive stimuli that could be identified with the small regions of the retina that maintain normal spacing.

4.1. Comparison of acuity to anatomical estimates of retinal sampling

Our retinal acuity results indicate that there is an underlying acuity deficit in myopia, which is most likely of neural origin. The comparison of angular and retinal acuity in Fig. 4 implies that the enlarged retinal image in an elongated myopic eye compensates for the neural acuity deficit, so that angular acuity nearly reaches the level of that in an emmetropic eye. The neural effects on acuity could involve a number of factors, such as an abnormality in the cones or inner retina, as well as retinal stretching. Several studies have shown that ERG amplitudes are reduced as axial length increases (Chan & Mohidin, 2003; Chen et al., 1992; Kawabata & Adachi-Usami, 1997; Pallin, 1969; Westall et al., 2001) and this effect is evident even in eyes with axial lengths less than 25 mm (Hidajat et al., 2003). There is also evidence for decreased retinal and choroidal blood flow in myopia (Reiner, Shih, & Fitzgerald, 1995; Shimada et al., 2004). Reiner et al. (1995) hypothesized that axial elongation in myopia leads to decreased choroidal blood flow, which in turn leads to ischemic outer retinal cell loss and hence losses in visual function. Disruptions in choroidal blood flow decrease visual acuity in pigeons (Hodos et al., 1998) and there is a correlation between the age-related declines in choroidal blood flow and visual acuity in pigeons (Fitzgerald et al., 2001). These abnormalities in retinal and choroidal function in myopia, even at a sub-clinical level, might be associated with changes in visual performance in human subjects. However it is well established that retinal stretching occurs in myopia (Curtin & Karlin, 1971), and stretching increases the spacing between adjacent rows of neurons and hence lowers spatial acuity (Bradley et al., 1983; Chui et al., 2005; Kramer et al., 1999; Romano & von Noorden, 1999; Strang et al., 1998; Winn et al., 1988).

Foveal interferometric acuity matches the Nyquist limit of the foveal cone mosaic (Green, 1970; Williams, 1985a; Williams & Coletta, 1987), while peripheral grating acuity is generally considered to be limited by the midget retinal ganglion cells that project to the parvocellular pathway (Anderson et al., 1992; Anderson, Mullen, & Hess, 1991; Dacey, 1993; Kolb & Marshak, 2003; Lennie & Fairchild, 1994; Merigan & Katz, 1990; Thibos et al., 1987; Wassle & Boycott, 1991). The retinal acuity values shown in Fig. 3B could therefore be considered as estimates of each subject's underlying neural sampling rate, and they are compared to anatomical estimates of human cone and midget ganglion cell spacing in Fig. 6. The anatomical data represent the row spacing, r, in μm, calculated from retinal cell density, d, in cells/mm^2, by $r = 1000 * (\sqrt{3}/2d)^{1/2}$ which assumes

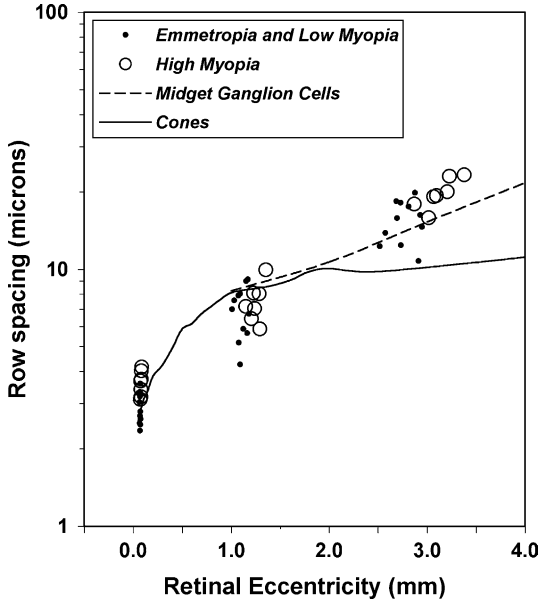

Fig. 6. Comparison of interferometric acuity to human cone and ganglion cell spacing. Acuity values in c/mm from Fig. 3B were converted to microns per half cycle and plotted against retinal eccentricity in mm. Each subject's acuity results are plotted at retinal eccentricities determined from the appropriate retinal magnification factor for the subject's refractive correction during acuity testing. Filled symbols are data from subjects with less than 6 D of myopia while open symbols are data from subjects with more than 6 D of myopia. Anatomical values are based on published cone and ganglion cell densities in human retina, and converted to microns per row, assuming a hexagonal mosaic. The solid line is the average cone spacing from 16 human eyes, gathered from the following studies: Curcio et al. (1990) (seven eyes; data from 0.05 to 4 mm retinal eccentricity temporal retina), Jonas et al. (1992) (six eyes; data from 0.04 to 2 mm eccentricity) and Sjostrand et al. (1999) (three eyes, data from 0.6 to 5 mm eccentricity with additional values for one eye from 0.03 to 1.8 mm published in Sjostrand et al. (1994)). The dashed line is the estimated average row spacing for half the population of the midget ganglion cells, assuming that the retinal image is sampled by independent mosaics of on- and off-type neurons arranged in hexagonal mosaics. Total ganglion cell counts were gathered from Curcio and Allen (1990) (average of five eyes, temporal retina). It was assumed that 95% of the total ganglion cells were the midget type for retinal eccentricities up to 4 mm.

that the neurons are arranged in hexagonal mosaics.[4] The solid line is the average cone spacing from 16 human eyes, gathered from four studies (Curcio, Sloan, Kalina, & Hendrickson, 1990; Jonas, Schneider, & Naumann, 1992; Sjostrand, Conradi, & Klaren, 1994; Sjostrand, Olsson, Popovic, & Conradi, 1999). The dashed line in Fig. 6 is the estimated row spacing of the midget ganglion cells in the temporal retina. The midget cell data were estimated from total ganglion cell counts averaged from eight human eyes in the Curcio and Allen's (1990) study, assuming that midget cells make up 95% of the total ganglion cell population at these retinal locations (Dacey, 1993). Because there are both on-and off-type midget cells, it has been theorized that each cell type samples the retinal image as an independent mosaic (Lennie & Fairchild, 1994; Merigan & Katz, 1990). Thus, row spacing for the midget ganglion cells represents a sampling mosaic with half the density of the total midget cell population assuming that on- and off-type cells are approximately equal in number (Dacey, 1993).

A grating cycle at the acuity limit should cover two rows of the underlying cell mosaic, so retinal acuity values were converted from c/mm to μm per half cycle. Data for the seven subjects with myopia greater than 6 D (i.e., high myopia) are shown as open symbols while data for the remaining 11 subjects are shown as filled symbols (emmetropia and low myopia, i.e., myopia less than 6 D). Acuity data are plotted at retinal eccentricities in millimeters calculated from each individual's RMF value. Foveal acuity data are plotted at a retinal eccentricity that corresponds to 0.25 deg because cone density varies considerably at the very center of the foveola (Curcio et al., 1990) and the 1 deg foveal grating patch would have covered a retinal area up to 0.5 deg eccentricity. For statistical comparison of our subjects' acuity to cone spacing, we used the mean cone row spacing at a retinal eccentricity of 73 μm, which corresponds to 0.25 deg using our average RMF of 290 μ/deg. The mean cone row spacing at this retinal eccentricity is 2.89 μm ± 0.49 SD. For the subjects without high myopia, the sampling rate estimated from foveal acuity has a mean of 2.90 μm ± 0.41 SD, which is not significantly different from the anatomical cone spacing (t test, $p = 0.48$). However, the sampling rate estimated from foveal acuity in the high myopes has a mean of 3.62 μm ± 0.40 SD, which is significantly greater than the anatomical cone spacing (t test, $p = 0.0014$). Thus, the lower foveal retinal acuity in the high myopes is consistent with retinal stretching.

Retinal acuity for the 4 deg condition (about 1.2 mm retinal eccentricity) tended to be better than the anatomical cone spacing. One might be tempted to explain this effect as the result of poor fixation (i.e., our naive subjects attempting to look toward the actual stimulus rather than the fixation mark at 4 deg) but this 'supra-Nyquist' resolution effect has been demonstrated previously for interferometric acuity in the parafovea (Williams & Coletta, 1987). Furthermore, the phenomenon of supra-Nyquist resolution can be demonstrated with simulations of high frequency gratings that are sampled by parafoveal or irregular cone mosaics (Geller et al., 1992; Williams & Coletta, 1987). The average cone row spacing at this retinal location was estimated to be 8.36 μm ± 1.44 SD. The sampling rate estimated from the 4 deg retinal acuity has a mean of 6.93 μm ± 1.57 SD for the subjects without high myopia, and 7.50 μm ± 1.34 SD for the subjects with high myopia. Neither of the sampling rates estimated from acuity are significantly different from the anatomical cone row spacing (t tests, $p = 0.092$ for subjects without high myopia and $p = 0.195$ for subjects with high myopia), but the coarser mean sampling rate for the subjects with high myopia is suggestive of greater retinal stretching in the parafovea in myopia.

At about 3 mm retinal eccentricity (data from the 10 deg condition), acuity values for all subjects are worse the prediction from cone spacing and instead are more consistent with row spacing derived from half of the midget cell density. For statistical comparison to our subjects' acuity, we used ganglion cell density data available from four individual eyes in Curcio and Allen (1990) and from three eyes in Popovic and Sjostrand (2001). Data from the latter study were the effective ganglion cell densities that had been adjusted for lateral displacement from the cones. The average midget ganglion cell row spacing at 3 mm eccentricity calculated from these seven eyes was 16.76 μm ± 2.79 SD. In the subjects without high myopia, the sampling rate estimated from acuity had an average of 15.46 μm ± 2.92 SD, which was not statistically different ($p = 0.18$) from the midget cell row spacing. However, the sampling rate estimated from acuity in the high myopes was 19.82 μm ± 2.66 SD, which was significantly higher ($p = 0.029$) than the midget cell row spacing. Due to the higher RMF values in the highly myopic eyes, the 10 deg stimulus falls at a slightly greater retinal eccentricity than 3 mm (average of 3.12 mm). However, the retinal eccentricity would need to be close to 4 mm for the midget cell row spacing to increase to nearly 20 μm (Curcio & Allen, 1990). Thus, the estimated neural sampling rate in the highly myopic subjects implies that their acuity in the near periphery is also impaired by retinal stretching.

4.2. Model of retinal stretching in myopia

Most studies of ocular shape indicate that myopic eyes exhibit greater expansion in the axial, or anterior–

[4] Appendix A discusses the validity of this assumption when there is directional stretching of the cone mosaic.

posterior, direction than in the transverse or coronal direction, with the result that the retinal contour in myopia is shaped like a prolate ellipse rather than a sphere (Atchison et al., 2004; Curtin & Karlin, 1971; Logan, Gilmartin, Wildsoet, & Dunne, 2004; Meyer-Schwickerath & Gerke, 1984; Millodot, 1981; Mutti, Sholtz, Friedman, & Zadnik, 2000; Rempt, Hoogerheide, & Hoogenboom, 1971; Seidemann, Schaeffel, Guirao, Lopez-Gil, & Artal, 2002; Wildsoet, 1997). This model of eye growth in myopia is consistent with an expansion of the eye that occurs mainly at the posterior pole, as opposed to an overall spherical expansion of the globe. Support for this type of eye growth is also evident in previous studies of acuity in myopia. The global expansion model assumes that the retinal sampling rate in myopia increases at the same rate as the axial length because the posterior chamber circumference increases by the same factor as its diameter (Chui et al., 2005). Posterior pole expansion provided the best explanation for the reduction in acuity with myopia in the Strang et al.'s (1998) study. In Chui et al. (2005), the amount of myopia that caused peripheral acuity to drop by half from the emmetropic level corresponded to a 1.29-fold increase in axial length. Thus, the inferred retinal sampling rate increased at a faster rate than the axial length, which is inconsistent with uniform spherical expansion of the globe.

Fig. 7 illustrates that interferometric retinal acuity also decreases with myopia at a faster rate than the prediction from uniform global expansion, and provides an estimate of the distance from which the posterior pole expands. For the global expansion model, the emmetropic eye was assumed to have a 22 mm diameter spherical posterior chamber, based on our data in Fig. 1A. The actual axial length for the emmetropic eye is 22.6 mm, but it was assumed that the anterior vertex of the schematic eye is positioned 0.6 mm in front of the posterior chamber.[5] Retinal acuity for the emmetropic eye ($\text{acuity}_{\text{emm}}$) was assumed to be 182 c/mm at the fovea and 35 c/mm at 10 deg eccentricity, based on Fig. 3B. Assuming no change in the anterior optics with changes in axial length and that the retinal sampling rate increases proportionally with axial length, acuity in c/mm can be predicted from the following relationship to axial length (AL) in mm:

$$\text{acuity} = (22 * \text{acuity}_{\text{emm}})/(\text{AL} - 0.6). \quad (7)$$

Predicted acuity values for the global expansion model are plotted in Fig. 7 against the model eye's refraction, which was converted from axial length by linear regression of the biometric data in Fig. 1A. Results for the fovea and for 10 deg eccentricity are shown in Figs. 7A and B, respectively. The retinal acuity of our subjects (solid symbols) decreases with myopia at a faster rate than the prediction from uniform global expansion (dotted line). Variation of the emmetropic posterior chamber diameter to values slightly smaller than 22 mm did not provide better simulations of the acuity data.

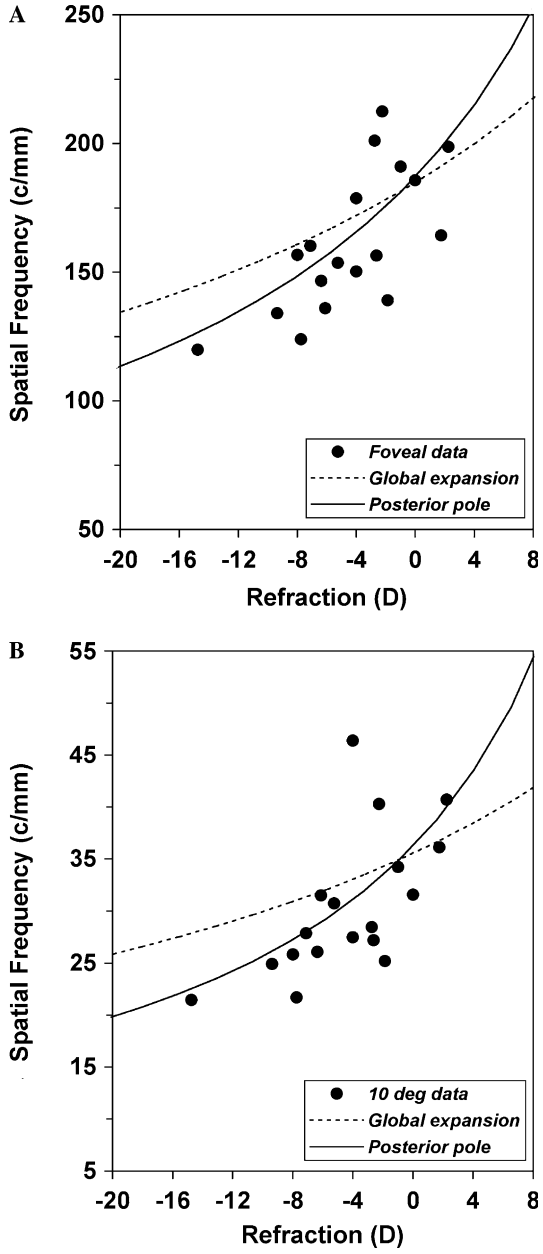

Fig. 7. Retinal acuity in c/mm at the fovea (A) and at 10 deg eccentricity (B) plotted against distance spherical equivalent refraction in Diopters, and compared to two models of global expansion in myopia, after Strang et al. (1998). The models assume an emmetropic acuity value of 182 c/mm for the fovea and 35 c/mm for 10 deg eccentricity; these values are the y-intercepts of the linear regressions to retinal acuity in Fig. 3B. Dotted curve is the model for uniform global expansion of a 22 mm spherical posterior chamber; solid curve is a least-squares fit to the acuity data of a model for expansion of the posterior pole (see text for details).

[5] The average anterior chamber depth of our subjects was 3 mm; a 2.4 mm sagittal depth into the 22 mm posterior chamber would result in a "limbal" diameter of the schematic eye of about 14 mm.

The alternative model of eye growth in Fig. 7, the posterior pole model, assumes the posterior section of the globe expands spherically from a point located at a distance x, in mm, in front of the emmetropic retina (Chui et al., 2005; Strang et al., 1998). Assuming an emmetropic eye with 22.6 mm axial length, the radius of the posterior pole sphere in the expanded eye would be x' which can be calculated from the expanded eye's axial length (AL) by subtracting the difference between 22.6 and x. The effect of posterior pole expansion on acuity in c/mm can be predicted from the emmetropic acuity and the axial length by the following formula:

$$\text{acuity} = (x * \text{acuity}_{\text{emm}})/(AL - (22.6 - x)). \quad (8)$$

The global expansion model in Eq. (7) is thus a special case of this model in which x is constrained to be 22 mm. The value of x for the posterior pole model was obtained from a least-squares curve fit of Eq. (8) to the retinal acuity data. Curve fits for both retinal locations (solid lines in Fig. 7) achieved r coefficients of 0.56, and the values obtained for x were 12.9 and 10.2 mm from the foveal and 10 deg data, respectively. The slightly shorter value of x obtained from the 10 deg data implies that retinal stretching may be slightly greater in the peripheral location than in the fovea. Our data at the fovea and at 10 deg eccentricity did not show appreciably different slopes on logarithmic scales (Fig. 3), but the values of myopia at which retinal acuity in c/mm would be halved from emmetropic acuity ($K2$ value in Chui et al., 2005), are −19.91 D in the fovea and −17.3 D at 10 deg eccentricity. Similarly, foveal acuity was halved by a 1.36 times increase in axial length, while peripheral acuity was halved by a 1.29 times increase in axial length. Thus interferometric retinal acuity suggests that the amount of retinal stretching could be slightly greater in the near periphery than in the fovea, which would be consistent with recent studies (Chui et al., 2005; Vera-Diaz et al., 2005).

5. Summary

Myopia does not cause a significant reduction in interferometric acuity, when it is compensated for the minifying effect of spectacles and expressed in angular units, such as cycles/deg. Myopes have significantly greater retinal image magnification than emmetropes, due to the increased axial length in myopia, and we find that retinal image magnification persists slightly in high myopia even with spectacle correction. When angular acuity is converted to retinal units of cycles/mm, myopic subjects have significantly lower acuity in the fovea and near periphery. Retinal acuity implies that highly myopic (>6 D) subjects have larger retinal sampling distances than published values of the spacing of human retinal neurons. Overall, these results indicate that a highly myopic eye has retinal neurons that are more widely spaced than normal, but the increased axial length enlarges the retinal image enough to compensate for the retinal stretching. The acuity data support a model of retinal stretching in myopia in which the globe expands primarily in the posterior pole area.

Acknowledgments

Support was provided by NIH Grants RO1 EY012847, T35 EY007149 and R24 EY014817.

Appendix A

We assumed that anatomical mosaics were hexagonal when we derived row spacing from density counts but there is evidence that cone mosaics are anisotropic, i.e., they are stretched in one direction. Parafoveal cones in the human retina have greater spacing radially than tangentially by 10–15% (Curcio & Sloan, 1992) and aliasing patterns of high frequency interference fringes indicate that foveal cone row spacing is 14% larger for vertical fringes than it is for horizontal fringes (Williams, 1988). Below we show that if one calculates row spacing from the lowered density after stretching, assuming 'erroneously' that the mosaic is still hexagonal, the calculated row spacing is about the same as the actual mean row spacing of the three main axes of the stretched mosaic.

Fig. 8 shows a simulated hexagonal cone mosaic (upper) and the same mosaic (lower) after it has been

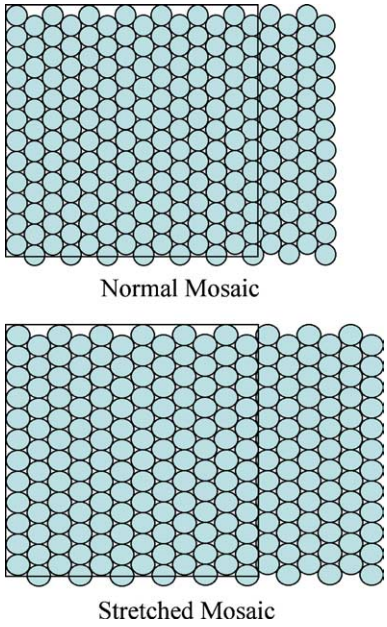

Fig. 8. Simulated cone mosaics before (upper) and after (lower) stretching by 15% in the horizontal direction. The square box simulates 1 mm^2.

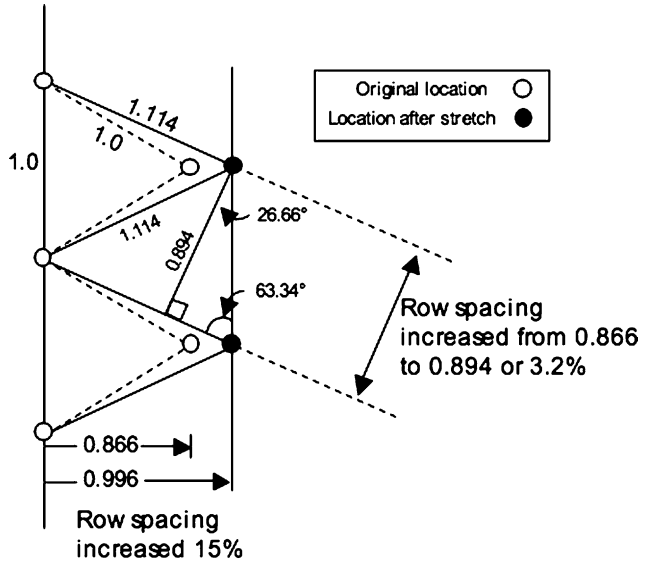

Fig. 9. Geometry of a hexagonal cone mosaic before and after stretching horizontally by 15%. Here the center to center cone spacing is assumed to be a unit-less value of 1. The figure shows the positions of the cone centers before stretching (white circles) with row spacing of 0.866. After stretching 15% in the horizontal direction, the positions of the two cone centers on the right are shown in black. The center to center spacing increases to 1.114 on two sides of each triangle while it remains 1 in the vertical direction since there was no stretching in that direction. The horizontal row spacing increases to 0.996 while row spacing of the other two main axes increases to 0.894 (sine of 63.34 deg). Thus the mean row spacing after stretching is 0.928 or about 7% larger than the row spacing before stretching. The orientation of the lattice does not affect the mean row spacing after horizontal stretching. If the mosaic had one of its main axes oriented horizontally, instead of vertically as shown, and was stretched by 15% in the horizontal direction, the vertical row spacing would be 0.866 before and after stretching, while the row spacing of the other two main axes would increase to 0.958, which yields a mean row spacing of 0.927, or again, about 7% larger than the row spacing before stretching.

stretched by 15% in the horizontal direction. The anatomical data that we used for comparison to our acuity are provided in terms of density per square millimeter. If the box lying over each mosaic represents a square millimeter, then the density before stretching[6] is 12×13.86 rows = 166.3 cones/mm^2 which is higher than the density after stretching, equal to 12×12.05 rows = 144.6 cones/mm^2. (These figures are not meant to match real anatomical data but are just for illustration). Assuming hexagonal packing, the row spacing calculated from the density is 72.16 μm/row for the normal mosaic and 77.39 μm/row for the stretched mosaic, which is about 7.2% larger (square root of the stretch factor). The actual horizontal row spacing of the stretched mosaic is 15% greater than in the original mosaic, or 1000/12.05 = 83 μm/row. So the assumption of hexagonal packing will underestimate the row spacing of the mosaic in the direction of the stretching. However the stretched mosaic still maintains three main axes of cones and the other two axes have not stretched as much as the horizontal axis. The other two main axes of the stretched mosaic each have a row spacing of 74.5 μm/row (only 3.2% larger than in the normal mosaic; see geometry in Fig. 9). The fact that, in the stretched mosaic, the row spacing of the other main axes is smaller than 83 μm/row means that grating stimuli with smaller half-cycle widths than 83 μm could be resolved. Taking the mean row spacing of the three main axes of the mosaic will yield 77.33 μm/row which is very close to the 77.39 μm/row calculated from the density above.

In summary, if there is directional stretching, an assumption of hexagonal packing will capture the overall increase in row spacing of the stretched mosaic. It is only when comparisons are being made along the direction of stretching that the hexagonal packing assumption will underestimate the stretched row spacing. Since our resolution data did not show any evidence that myopes have additional directional stretching compared to emmetropes, then it is valid to compare our acuity data (averaged for both vertical and horizontal orientations) to the row spacing calculated from anatomical density, assuming hexagonal packing.

[6] Twelve is $\sqrt{3}/2$ smaller than 13.86 and 12.05 is 15% less than 13.86.

References

Anderson, R. S., Wilkinson, M. O., & Thibos, L. N. (1992). Psychophysical localization of the human visual streak. *Optometry and Vision Science, 69*, 171–174.

Anderson, S. J., Mullen, K. T., & Hess, R. F. (1991). Human peripheral spatial resolution for achromatic and chromatic stimuli: Limits imposed by optical and retinal factors. *Journal of Physiology, 442*, 47–64.

Applegate, R. A. (1991). Monochromatic wavefront aberrations in myopia. In *Vision science and its applications. Tech. digest series* (Vol. 2, pp. 234–237). Washington, DC: Optical Society of America.

Applegate, R. A., & Howland, H. C. (1993). Magnification and visual acuity in refractive surgery. *Archives of Ophthalmology, 111*, 1335–1342.

Atchison, D. A., Jones, C. E., Schmid, K. L., Pritchard, N., Pope, J. M., Strugnell, W. E., et al. (2004). Eye shape in emmetropia and myopia. *Investigative Ophthalmology & Visual Science, 45*, 3380–3386.

Atchison, D. A., Scott, D. H., & Charman, W. N. (2003). Hartmann–Shack technique and refraction across the horizontal visual field. *Journal of the Optical Society of America A, 20*, 965–973.

Bennett, A. G. (1988). A method of determining the equivalent powers of the eye and its crystalline lens without resort to phakometry. *Ophthalmic and Physiological Optics, 8*, 53–59.

Bennett, A. G., & Rabbetts, R. B. (1998). Clinical visual optics (3rd ed.). Boston: Butterworth-Heinemann.

Bradley, A., Rabin, J., & Freeman, R. D. (1983). Nonoptical determinants of aniseikonia. *Investigative Ophthalmology & Visual Science, 24*, 507–512.

Campbell, F. W., & Green, D. G. (1965). Optical and retinal factors affecting visual resolution. *Journal of Physiology, 181*, 576–593.

Carkeet, A., Luo, H. D., Tong, L., Saw, S. M., & Tan, D. T. (2002). Refractive error and monochromatic aberrations in Singaporean children. *Vision Research, 42*, 1809–1824.

Carney, L. G., Mainstone, J. C., & Henderson, B. A. (1997). Corneal topography and myopia. A cross-sectional study. *Investigative Ophthalmology & Visual Science, 38*, 311–320.

Chan, H. L., & Mohidin, N. (2003). Variation of multifocal electroretinogram with axial length. *Ophthalmic Physiology and Optics, 23*, 133–140.

Chen, J., Elsner, A., Burns, S. A., Hansen, R. M., Lou, P. L., Kwong, K. K., et al. (1992). The effect of eye shape on retinal responses. *Clinical and Vision Science, 7*, 521–530.

Cheng, X., Bradley, A., Hong, X., & Thibos, L. N. (2003). Relationship between refractive error and monochromatic aberrations of the eye. *Optometry and Vision Science, 80*, 43–49.

Cheng, X., Bradley, A., & Thibos, L. N. (2004). Predicting subjective judgment of best focus with objective image quality metrics. *Journal of Vision, 4*, 310–321.

Chui, T. Y. P., Yap, M. K. H., Chan, H. H. L., & Thibos, L. N. (2005). Retinal stretching limits peripheral visual acuity in myopia. *Vision Research, 45*, 593–605.

Coletta, N. J., Marcos, S., Wildsoet, C., & Troilo, D. (2003). Double-pass measurement of retinal image quality in the chicken eye. *Optometry and Vision Science, 80*, 50–57.

Coletta, N. J., & Moskowitz, A. (2003). Wavefront aberrations and mesopic visual performance following soft contact lens removal. *Journal of Vision, 3*(12), 37a.

Coletta, N. J., & Sharma, V. (1995). Effects of luminance and spatial noise on interferometric contrast sensitivity. *Journal of the Optical Society of America A, 12*, 2244–2251.

Collins, J. W., & Carney, L. G. (1990). Visual performance in high myopia. *Current Eye Research, 9*, 217–223.

Collins, M. J., Wildsoet, C. F., & Atchison, D. A. (1995). Monochromatic aberrations and myopia. *Vision Research, 35*, 1157–1163.

Comerford, J. P., Thorn, F., & Corwin, T. R. (1987). Effect of luminance level on contrast sensitivity in myopia. *American Journal of Optometry and Physiological Optics, 64*, 810–814.

Curcio, C. A., & Allen, K. A. (1990). Topography of ganglion cells in human retina. *Journal of Comparative Neurology, 300*, 5–25.

Curcio, C. A., & Sloan, K. R. (1992). Packing geometry of human cone photoreceptors: Variation with eccentricity and evidence for local anisotropy. *Visual Neuroscience, 9*, 169–180.

Curcio, C. A., Sloan, K. R., Kalina, R. E., & Hendrickson, A. E. (1990). Human photoreceptor topography. *Journal of Comparative Neurology, 292*, 497–523.

Curtin, B. J. (1985). In *The myopias, basic science and clinical management* (pp. 17–27). Philadelphia, PA: Harper & Row.

Curtin, B. J., & Karlin, D. B. (1971). Axial length measurements and fundus changes of the myopic eye. *American Journal of Ophthalmology, 1*, 42–53.

Dacey, D. M. (1993). The mosaic of midget ganglion cells in the human retina. *Journal of Neuroscience, 13*, 5334–5355.

Dorronsoro, C., Barbero, S., Llorente, L., & Marcos, S. (2003). On-eye measurement of optical performance of rigid gas permeable contact lenses based on ocular and corneal aberrometry. *Optometry and Vision Science, 80*, 115–125.

Doughty, M. J., & Zaman, M. L. (2000). Human corneal thickness and its impact on intraocular pressure measures: A review and meta-analysis approach. *Survey of Ophthalmology, 44*, 367–408.

Drasdo, N., & Fowler, C. W. (1974). Non-linear projection of the retinal image in a wide-angle schematic eye. *British Journal of Ophthalmology, 58*, 709–714.

Dunne, M. C., Barnes, D. A., & Royston, J. M. (1989). An evaluation of Bennett's method for determining the equivalent powers of the eye and its crystalline lens without resort to phakometry. *Ophthalmic and Physiological Optics, 9*, 69–71.

Fiorentini, A., & Maffei, L. (1976). Spatial contrast sensitivity of myopic subjects. *Vision Research, 16*, 437–438.

Fitzgerald, D. E., Chung, I., & Krumholtz, I. (2005). An analysis of high myopia in a pediatric population less than10 years of age. *Optometry, 76*, 102–114.

Fitzgerald, M. E., Tolley, E., Frase, S., Zagvazdin, Y., Miller, R. F., Hodos, W., et al. (2001). Functional and morphological assessment of age-related changes in the choroid and outer retina in pigeons. *Visual Neuroscience, 18*, 299–317.

Frisen, L., & Frisen, M. (1976). A simple relationship between the probability distribution of visual acuity and the density of retinal output channels. *Acta Ophthalmologica, 54*, 437–444.

Frisen, L., & Glansholm, A. (1975). Optical and neural resolution in peripheral vision. *Investigative Ophthalmology, 14*, 528–536.

Geddes, L. A., Patel, B. J., & Bradley, A. (1990). Comparison of Snellen and interferometer visual acuity in an aging noncataractous population. *Optometry and Vision Science, 67*, 361–365.

Geller, A. M., Sieving, P. A., & Green, D. G. (1992). Effect on grating identification of sampling with degenerate arrays. *Journal of the Optical Society of America A, 9*, 472–477.

Goss, D. A., Cox, V. D., Herrin-Lawson, G. A., Nielsen, E. D., & Dolton, W. A. (1990). Refractive error, axial length, and height as a function of age in young myopes. *Optometry and Vision Science, 67*, 332–338.

Green, D. G. (1970). Regional variations in the visual acuity for interference fringes on the retina. *Journal of Physiology, 207*, 351–356.

Grosvenor, T., & Scott, R. (1994). Role of the axial length/corneal radius ratio in determining the refractive state of the eye. *Optometry and Vision Science, 71*, 573–579.

He, J. C., Sun, P., Held, R., Thorn, F., Sun, X., & Gwiazda, J. E. (2002). Wavefront aberrations in eyes of emmetropic and moderately myopic school children and young adults. *Vision Research, 42*, 1063–1070.

Hess, R. F., Dakin, S. C., & Kapoor, N. (2000). The foveal 'crowding' effect: physics or physiology. *Vision Research, 40*(4), 365–370.

Hidajat, R., Mclay, J., Burley, C., Elder, M., Morton, J., & Goode, D. (2003). Influence of axial length of normal eyes on PERG. *Documenta Ophthalmologica, 107*, 195–200.

Hodos, W., Miller, R. F., Ghim, M. M., Fitzgerald, M. E., Toledo, C., & Reiner, A. (1998). Visual acuity losses in pigeons with lesions of the nucleus of Edinger–Westphal that disrupt the adaptive regulation of choroidal blood flow. *Visual Neuroscience, 15*, 273–287.

Holden, A. L., & Fitzke, F. W. (1988). Image size in the fundus: Structural evidence for wide-field retinal magnification factor. *British Journal of Ophthalmology, 72*, 228–230.

Hong, X., Himebaugh, N., & Thibos, L. N. (2001). On-eye evaluation of optical performance of rigid and soft contact lenses. *Optometry and Vision Science, 78*, 872–880.

Jonas, J. B., Schneider, U., & Naumann, G. O. (1992). Count and density of human retinal photoreceptors. *Graefe's Archive for Clinical and Experimental Ophthalmology, 230*, 505–510.

Kawabata, H., & Adachi-Usami, E. (1997). Multifocal electroretinogram in myopia. *Investigative Ophthalmology & Visual Science, 38*, 2844–2851.

Kolb, H., & Marshak, D. (2003). The midget pathways of the primate retina. *Documenta Ophthalmologica, 106*, 67–81.

Kramer, P., Shippman, S., Bennett, G., Meininger, D., & Lubkin, V. (1999). A study of aniseikonia and Knapp's law using a projection space eikonometer. *Binocular Vision & Strabismus Quarterly, 14*, 197–201.

Laws, F., Laws, D., Wood, I., & Clark, D. (1998). Assessment of a new through-the-eyelid technique for 'A' scan ultrasound ocular axial length measurement. *Ophthalmic and Physiological Optics, 18*, 408–414.

Lennie, P., & Fairchild, M. D. (1994). Ganglion cell pathways for rod vision. *Vision Research, 34*, 477–482.

Liou, S. W., & Chiu, C. J. (2001). Myopia and contrast sensitivity function. *Current Eye Research, 22*, 81–84.

Llorente, L., Barbero, S., Cano, D., Dorronsoro, C., & Marcos, S. (2004). Myopic versus hyperopic eyes: Axial length, corneal shape and optical aberrations. *Journal of Vision, 4*, 288–298.

Logan, N. S., Gilmartin, B., Wildsoet, C. F., & Dunne, M. C. (2004). Posterior retinal contour in adult human anisomyopia. *Investigative Ophthalmology & Visual Science, 45*, 2152–2162.

Lu, F., Mao, X., Qu, J., Xu, D., & He, J. C. (2003). Monochromatic wavefront aberrations in the human eye with contact lenses. *Optometry and Vision Science, 80*, 135–141.

Marcos, S., Moreno-Barriuso, E., Llorente, L., Navarro, R., & Barbero, S. (2000). Do myopic eyes suffer from larger amount of aberrations? *Myopia 2000: Proceedings of the VIII International Conference on Myopia*, Boston: pp. 118–121.

Marsack, J. D., Thibos, L. N., & Applegate, R. A. (2004). Metrics of optical quality derived from wave aberrations predict visual performance. *Journal of Vision, 4*, 322–328.

Merigan, W. H., & Katz, L. M. (1990). Spatial resolution across the macaque retina. *Vision Research, 30*, 985–991.

Meyer-Schwickerath, G., & Gerke, E. (1984). Biometric studies of the eyeball and retinal detachment. *British Journal of Ophthalmology, 68*, 29–31.

Millodot, M. (1981). Effect of ametropia on peripheral refraction. *American Journal of Optometry and Physiological Optics, 5*, 691–695.

Morad, Y., Werker, E., & Nemet, P. (1999). Visual acuity tests using chart, line, and single optotype in healthy and amblyopic children. *Journal of the American Association of Pediatric Ophthalmology and Strabismus, 3*, 94–97.

Mutti, D. O., Sholtz, R. I., Friedman, N. E., & Zadnik, K. (2000). Peripheral refraction and ocular shape in children. *Investigative Ophthalmology & Visual Science, 41*, 1022–1030.

Pallin, O. (1969). The influence of the axial size of the eye on the size of the recorded b-potential in the clinical single-flash electroretinogram. *Acta Ophthalmologica, 191*(Suppl.), 1–57.

Paquin, M. P., Hamam, H., & Simonet, P. (2002). Objective measurement of optical aberrations in myopic eyes. *Optometry and Vision Science, 79*, 285–291.

Pesudovs, K., & Weisinger, H. S. (2004). A comparison of autorefractor performance. *Optometry and Vision Science, 81*, 554–558.

Popovic, Z., & Sjostrand, J. (2001). Resolution, separation of retinal ganglion cells, and cortical magnification in humans. *Vision Research, 41*, 1313–1319.

Porter, J., Guirao, A., Cox, I. G., & Williams, D. R. (2001). Monochromatic aberrations of the human eye in a large population. *Journal of the Optical Society of America A, 18*, 1793–1803.

Reiner, A., Shih, Y. F., & Fitzgerald, M. E. (1995). The relationship of choroidal blood flow and accommodation to the control of ocular growth. *Vision Research, 35*, 1227–1245.

Rempt, F., Hoogerheide, J., & Hoogenboom, W. P. (1971). Peripheral retinoscopy and the skiagram. *Ophthalmologica, 162*, 1–10.

Romano, P. E. (1988). The cause of organic amblyopia in high myopia. *Ophthalmology, 95*, 288.

Romano, P. E., & von Noorden, G. K. (1999). Knapp's law and unilateral axial high myopia. *Binocular Vision & Strabismus Quarterly, 14*, 215–222.

Royston, J. M., Dunne, M. C. M., & Barnes, D. A. (1989). Calculation of crystalline lens radii without resort to phakometry. *Ophthalmic and Physiological Optics, 9*, 412–414.

Seidemann, A., Schaeffel, F., Guirao, A., Lopez-Gil, N., & Artal, P. (2002). Peripheral refractive errors in myopic, emmetropic, and hyperopic young subjects. *Journal of the Optical Society of America A, 19*, 2363–2373.

Shimada, N., Ohno-Matsui, K., Harino, S., Yoshida, T., Yasuzumi, K., Kojima, A., et al. (2004). Reduction of retinal blood flow in high myopia. *Graefe's Archive for Clinical and Experimental Ophthalmology, 242*, 284–288.

Sjostrand, J., Conradi, N., & Klaren, L. (1994). How many ganglion cells are there to a foveal cone? A stereologic analysis of the quantitative relationship between cone and ganglion cells in one normal human fovea. *Graefe's Archive for Clinical and Experimental Ophthalmology, 232*, 432–437.

Sjostrand, J., Olsson, V., Popovic, Z., & Conradi, N. (1999). Quantitative estimations of foveal and extra-foveal retinal circuitry in humans. *Vision Research, 39*, 2987–2998.

Strang, N. C., Winn, B., & Bradley, A. (1998). The role of neural and optical factors in limiting visual resolution in myopia. *Vision Research, 38*, 1713–1721.

Thibos, L. N., Cheney, F. E., & Walsh, D. J. (1987). Retinal limits to the detection and resolution of gratings. *Journal of the Optical Society of America A, 4*, 1524–1529.

Thorn, F., Corwin, T. R., & Comerford, J. P. (1986). High myopia does not affect contrast sensitivity. *Current Eye Research, 5*, 635–639.

Troilo, D. (1998). Changes in retinal morphology following experimentally induced myopia. In *Vision science and its applications. Tech. digest series* (Vol. 1, pp. 206–209). Washington, DC: Optical Society of America.

Tunnacliffe, A. H. (1993). In *Introduction to visual optics* (pp. 42–65). London: Association of British Dispensing Opticians, 79–82.

Tunnacliffe, A. H., & Hirst, J. G. (1996). In *Optics* (2nd ed., pp. 130–132). London: Association of British Dispensing Opticians.

Van Alphen, G. W. H. M. (1961). On emmetropia and ametropia. *Ophthalmologica, 142*(Suppl.), 1–92.

Vera-Diaz, F. A., McGraw, P. V., Strang, N. C., & Whitaker, D. (2005). A psychophysical investigation of ocular expansion in human eyes. *Investigative Ophthalmology & Visual Science, 46*, 758–763.

Wassle, H., & Boycott, B. B. (1991). Functional architecture of the mammalian retina. *Physiological Review, 71*, 447–480.

Westall, C. A., Dhaliwal, H. S., Panton, C. M., Sigesmun, D., Levin, A. V., Nischal, K. K., & Heon, E. (2001). Values of electroretinogram responses according to axial length. *Documenta Ophthalmologica, 102*, 115–130.

Wildsoet, C. F. (1997). Active emmetropization—evidence for its existence and ramifications for clinical practice. *Ophthalmic Physiology and Optics, 17*, 279–290.

Williams, D. R. (1985a). Visibility of interference fringes near the resolution limit. *Journal of the Optical Society of America A, 2*, 1087–1093.

Williams, D. R. (1985b). Aliasing in human foveal vision. *Vision Research, 25*, 195–205.

Williams, D. R. (1988). Topography of the foveal cone mosaic in the living human eye. *Vision Research, 28*, 433–454.

Williams, D. R., & Coletta, N. J. (1987). Cone spacing and the visual resolution limit. *Journal of the Optical Society of America A, 4*, 1514–1523.

Winn, B., Ackerley, R. G., Brown, C. A., Murray, F. K., Prais, J., & St. John, M. F. (1988). Reduced aniseikonia in axial anisometropia with contact lens correction. *Ophthalmic and Physiological Optics, 8*, 341–344.